

# Signal of right-handed currents using $B \rightarrow K^* \ell^+ \ell^-$ observables at the kinematic endpoint.

Anirban Karan,<sup>1</sup> Rusa Mandal,<sup>1</sup> Abinash Kumar Nayak,<sup>1</sup> Rahul Sinha,<sup>1</sup> and Thomas E. Browder<sup>2</sup>

<sup>1</sup>*The Institute of Mathematical Sciences, HBNI, Taramani, Chennai 600113, India*

<sup>2</sup>*Department of Physics and Astronomy, University of Hawaii, Honolulu, HI 96822, USA*

(Dated: May 4, 2022)

The decay mode  $B \rightarrow K^* \ell^+ \ell^-$  is one of the most promising modes to probe physics beyond the standard model (SM), since the angular distribution of the decay products enable measurement of several constraining observables. LHCb has recently measured these observables using  $3 \text{ fb}^{-1}$  of data as a binned function of  $q^2$ , the dilepton invariant mass squared. We find that LHCb data implies evidence for right-handed currents, which are absent in the SM. These conclusions are derived in the maximum  $q^2$  limit and are free from hadronic corrections. Our approach differs from other approaches that probe new physics at low  $q^2$  as it does not require estimates of hadronic parameters but relies instead on heavy quark symmetries that are reliable at the maximum  $q^2$  kinematic endpoint.

PACS numbers: 11.30.Er, 13.25.Hw, 12.60.-i

The rare decay  $B \rightarrow K^* \ell^+ \ell^-$ , which involves a  $b \rightarrow s$  flavor changing loop induced quark transition at the quark level, provides an indirect but very sensitive probe of new physics (NP) beyond the standard model (SM). The angular distribution of the decay products provides a large number of observables [1] and thus can be used to reduce hadronic uncertainties making the mode a very special tool to probe for NP. Significant work has been done to probe NP in this mode. Most previous attempts have focused [2] on the low dilepton invariant mass squared region  $q^2 = 1 - 6 \text{ GeV}^2$ . An alternative approach that probes the maximum  $q^2$  limit has also been studied in literature [3, 4]. We show that this limit holds significant promise for clean probes of NP. A previous study suggested a possible signal of NP in the large  $q^2$  region [5]. In this letter we show that LHCb data implies a  $5\sigma$  signal for the existence of NP. While the evidence for right handed currents is clear, other NP contributions are also possible. Our conclusions are derived in the maximum  $q^2$  limit ( $q_{\text{max}}^2$ ) and are free from hadronic corrections. Our approach differs from other approaches that probe NP at low  $q^2$  by not requiring estimates of hadronic parameters but relying instead on heavy quark symmetries that are highly reliable at the kinematic endpoint  $q_{\text{max}}^2$  [3, 6]. While the observables themselves remain unaltered from their SM values, their derivatives and second derivatives at the endpoint are sensitive to NP effects.

The decay  $B \rightarrow K^* \ell^+ \ell^-$  is described by six transversity amplitudes that can be written as [7]

$$\mathcal{A}_{\lambda}^{L,R} = C_{L,R}^{\lambda} \mathcal{F}_{\lambda} - \tilde{\mathcal{G}}_{\lambda} = (\tilde{C}_9^{\lambda} \mp C_{10}) \mathcal{F}_{\lambda} - \tilde{\mathcal{G}}_{\lambda} \quad (1)$$

within the standard model in the massless lepton limit [8]. This parametric form of the amplitude is general enough to comprehensively include all short-distance and long-distance effects, factorizable and nonfactorizable contributions, resonance contributions and complete electromagnetic corrections to hadronic operators up to

all orders. In Eq. (1)  $C_9$  and  $C_{10}$  are Wilson coefficients with  $\tilde{C}_9^{\lambda}$  being the redefined “effective” Wilson coefficient defined [7, 9, 10] as

$$\tilde{C}_9^{\lambda} = C_9 + \Delta C_9^{(\text{fac})}(q^2) + \Delta C_9^{\lambda,(\text{non-fac})}(q^2) \quad (2)$$

where  $\Delta C_9^{(\text{fac})}(q^2)$ ,  $\Delta C_9^{\lambda,(\text{non-fac})}(q^2)$  correspond to factorizable and soft gluon non-factorizable contributions. The Wilson coefficient  $C_{10}$  is unaffected by strong interaction effects coming from electromagnetic corrections to hadronic operators [11]. The form factors  $\mathcal{F}_{\lambda}$  and  $\tilde{\mathcal{G}}_{\lambda}$  introduced in Eq. (1) can be related to the conventional form factors describing the decay as shown in the appendix of Ref. [7].

In the SM,  $\mathcal{F}_{\lambda}$ ’s and  $C_{10}$  are real, whereas  $\tilde{C}_9^{\lambda}$  and  $\tilde{\mathcal{G}}_{\lambda}$  contain the imaginary contributions of the amplitudes. Defining two variables  $r_{\lambda}$  and  $\varepsilon_{\lambda}$ , the amplitudes  $\mathcal{A}_{\lambda}^{L,R}$  in Eq. (1) can be rewritten as,

$$\mathcal{A}_{\lambda}^{L,R} = (\mp C_{10} - r_{\lambda}) \mathcal{F}_{\lambda} + i \varepsilon_{\lambda}, \quad (3)$$

where

$$r_{\lambda} = \frac{\text{Re}(\tilde{\mathcal{G}}_{\lambda})}{\mathcal{F}_{\lambda}} - \text{Re}(\tilde{C}_9^{\lambda}), \quad (4)$$

$$\varepsilon_{\lambda} = \text{Im}(\tilde{C}_9^{\lambda}) \mathcal{F}_{\lambda} - \text{Im}(\tilde{\mathcal{G}}_{\lambda}). \quad (5)$$

The observables  $F_{\perp}$ ,  $F_{\parallel}$ ,  $F_L$ ,  $A_{\text{FB}}$  and  $A_5$  are defined as,

$$F_{\lambda} = \frac{|\mathcal{A}_{\lambda}^L|^2 + |\mathcal{A}_{\lambda}^R|^2}{\Gamma_f} \quad \lambda \in \{\perp, \parallel, 0\}, \quad (6)$$

$$A_{\text{FB}} = \frac{3}{2} \frac{\text{Re}(\mathcal{A}_{\parallel}^L \mathcal{A}_{\perp}^{L*} - \mathcal{A}_{\parallel}^R \mathcal{A}_{\perp}^{R*})}{\Gamma_f}, \quad (7)$$

$$A_5 = \frac{3}{2\sqrt{2}} \frac{\text{Re}(\mathcal{A}_0^L \mathcal{A}_{\perp}^{L*} - \mathcal{A}_0^R \mathcal{A}_{\perp}^{R*})}{\Gamma_f}, \quad (8)$$

where  $\Gamma_f \equiv \sum_{\lambda} (|\mathcal{A}_{\lambda}^L|^2 + |\mathcal{A}_{\lambda}^R|^2)$ . We neglect the  $\varepsilon_{\lambda}$  contributions to the amplitude for the time being, but will

include them later. In the presence of RH currents the transversity amplitudes are given by [11]

$$\mathcal{A}_{\perp}^{L,R} = ((\tilde{C}_9^{\perp} + C_9') \mp (C_{10} + C_{10}')) \mathcal{F}_{\perp} - \tilde{\mathcal{G}}_{\perp} \quad (9)$$

$$\mathcal{A}_{\parallel}^{L,R} = ((\tilde{C}_9^{\parallel} - C_9') \mp (C_{10} - C_{10}')) \mathcal{F}_{\parallel} - \tilde{\mathcal{G}}_{\parallel} \quad (10)$$

$$\mathcal{A}_0^{L,R} = ((\tilde{C}_9^0 - C_9') \mp (C_{10} - C_{10}')) \mathcal{F}_0 - \tilde{\mathcal{G}}_0. \quad (11)$$

Note that setting the RH contributions  $C_9'$  and  $C_{10}'$  to zero, the amplitudes reduce to the SM ones in Eq. (1).

Introducing new variables

$$\xi = \frac{C_{10}'}{C_{10}} \quad \text{and} \quad \xi' = \frac{C_9'}{C_{10}} \quad (12)$$

the observables  $F_{\perp}$ ,  $F_{\parallel}$ ,  $A_{\text{FB}}$ ,  $A_5$  (Eqs. (6) – (8)) can be expressed as,

$$F_{\perp} = 2\zeta(1 + \xi)^2(1 + R_{\perp}^2) \quad (13)$$

$$F_{\parallel} P_1^2 = 2\zeta(1 - \xi)^2(1 + R_{\parallel}^2) \quad (14)$$

$$F_L P_2^2 = 2\zeta(1 - \xi)^2(1 + R_0^2) \quad (15)$$

$$A_{\text{FB}} P_1 = 3\zeta(1 - \xi^2)(R_{\parallel} + R_{\perp}) \quad (16)$$

$$\sqrt{2}A_5 P_2 = 3\zeta(1 - \xi^2)(R_0 + R_{\perp}) \quad (17)$$

$$\text{where } P_1 = \frac{\mathcal{F}_{\perp}}{\mathcal{F}_{\parallel}}, \quad P_2 = \frac{\mathcal{F}_{\perp}}{\mathcal{F}_0}, \quad \zeta = \frac{\mathcal{F}_{\perp}^2 C_{10}^2}{\Gamma_f},$$

$$R_{\perp} = \frac{\frac{r_{\perp}}{C_{10}} - \xi'}{1 + \xi}, \quad R_{\parallel} = \frac{\frac{r_{\parallel}}{C_{10}} + \xi'}{1 - \xi}, \quad R_0 = \frac{\frac{r_0}{C_{10}} + \xi'}{1 - \xi}. \quad (18)$$

We consider the observables  $F_L$ ,  $F_{\parallel}$ ,  $F_{\perp}$ ,  $A_{\text{FB}}$  and  $A_5$ , with the constraint  $F_L + F_{\parallel} + F_{\perp} = 1$ . Using Eq. (13)–(17), we obtain expressions for  $R_{\perp}$ ,  $R_{\parallel}$ ,  $R_0$  and  $P_2$  in terms of the observables and  $P_1$ :

$$R_{\perp} = \pm \frac{3}{2} \frac{\left(\frac{1-\xi}{1+\xi}\right) F_{\perp} + \frac{1}{2} P_1 Z_1}{P_1 A_{\text{FB}}} \quad (19)$$

$$R_{\parallel} = \pm \frac{3}{2} \frac{\left(\frac{1+\xi}{1-\xi}\right) P_1 F_{\parallel} + \frac{1}{2} Z_1}{A_{\text{FB}}} \quad (20)$$

$$R_0 = \pm \frac{3}{2\sqrt{2}} \frac{\left(\frac{1+\xi}{1-\xi}\right) P_2 F_L + \frac{1}{2} Z_2}{A_5} \quad (21)$$

$$P_2 = \frac{\left(\frac{1-\xi}{1+\xi}\right) 2P_1 A_{\text{FB}} F_{\perp}}{\sqrt{2}A_5 \left( \left(\frac{1-\xi}{1+\xi}\right) 2F_{\perp} + Z_1 P_1 \right) - Z_2 P_1 A_{\text{FB}}} \quad (22)$$

where  $Z_1 = (4F_{\parallel}F_{\perp} - \frac{16}{9}A_{\text{FB}}^2)^{1/2}$  and  $Z_2 = (4F_L F_{\perp} - \frac{32}{9}A_5^2)^{1/2}$ . Since we have one extra parameter compared to observables, all the above expressions depend on  $P_1$ . Fortunately in the large  $q^2$  limit, the relations between form factors enable us to eliminate one parameter.

At the kinematic limit  $q^2 = q_{\text{max}}^2 = (m_B - m_{K^*})^2$  the  $K^*$  meson is at rest and the two leptons travel back to back in the  $B$  meson rest frame. There is no preferred

direction in the decay kinematics. Hence, the differential decay distribution in this kinematic limit must be independent of the angles  $\theta_{\ell}$  and  $\phi$ , which can be integrated out. This imposes constraints on the amplitude  $A_{\lambda}^{L,R}$  and hence the observables. The entire decay, including the decay  $K^* \rightarrow K\pi$  takes place in one plane, resulting in a vanishing contribution to the ' $\perp$ ' helicity, or  $F_{\perp} = 0$ . Since the  $K^*$  decays at rest, the distribution of  $K\pi$  is isotropic and cannot depend on  $\theta_K$ . It can easily be seen that this is only possible if  $F_{\parallel} = 2F_L$  [6].

At  $q^2 = q_{\text{max}}^2$ ,  $\Gamma_f \rightarrow 0$  as all the transversity amplitudes vanish in this limit. The constraints on the amplitudes described above result in unique values of the helicity fractions and the asymmetries at this kinematical endpoint. The values of the helicity fractions and asymmetries were derived in Ref. [6, 7] where it is explicitly shown that

$$F_L(q_{\text{max}}^2) = \frac{1}{3}, \quad F_{\parallel}(q_{\text{max}}^2) = \frac{2}{3}, \quad A_4(q_{\text{max}}^2) = \frac{2}{3\pi},$$

$$F_{\perp}(q_{\text{max}}^2) = 0, \quad A_{\text{FB}}(q_{\text{max}}^2) = 0, \quad A_{5,7,8,9}(q_{\text{max}}^2) = 0. \quad (23)$$

The large  $q^2$  region where the  $K^*$  has low-recoil energy has also been studied [3, 12] in a modified heavy quark effective theory framework. In the limit  $q^2 \rightarrow q_{\text{max}}^2$  the hadronic form factors satisfy the conditions

$$\frac{\tilde{\mathcal{G}}_{\parallel}}{\mathcal{F}_{\parallel}} = \frac{\tilde{\mathcal{G}}_{\perp}}{\mathcal{F}_{\perp}} = \frac{\tilde{\mathcal{G}}_0}{\mathcal{F}_0} = -\kappa \frac{2m_b m_B C_7}{q^2}, \quad (24)$$

where  $\kappa \approx 1$  as shown in [12] and at  $q_{\text{max}}^2$ , one defines  $r$  such that  $r_0 = r_{\parallel} = r_{\perp} \equiv r$  [13]. Therefore Eq. (18) implies that in the presence of RH currents one should expect  $R_0 = R_{\parallel} \neq R_{\perp}$  at  $q^2 = q_{\text{max}}^2$  without any approximation. Interestingly, this relation is unaltered by non-factorizable and resonance contributions [6] at this kinematic endpoint.

We study the values of  $R_{\lambda}$ ,  $\zeta$  and  $P_{1,2}$  in the large  $q^2$  region and consider the kinematic limit  $q^2 \rightarrow q_{\text{max}}^2$ . It is easy to see from Eq. (13) that  $F_{\perp}(q_{\text{max}}^2) = 0$  implies that  $\zeta = 0$  in the limit  $q^2 \rightarrow q_{\text{max}}^2$ . Further, since  $R_{\parallel}(q_{\text{max}}^2) = R_0(q_{\text{max}}^2)$ , Eqs. (14) and (15) imply that in the limit  $q^2 \rightarrow q_{\text{max}}^2$ ,  $P_2 = \sqrt{2}P_1$ . However, both  $P_1$  and  $P_2$  go to zero at  $q_{\text{max}}^2$ . It is therefore imperative that we take into account the limiting values very carefully by Taylor expanding all observables around the endpoint  $q_{\text{max}}^2$  in terms of the variable  $\delta \equiv q_{\text{max}}^2 - q^2$ . The leading power of  $\delta$  in the Taylor expansion must take into account the relative momentum dependence of the amplitudes  $\mathcal{A}_{\lambda}^{L,R}$ . Eq. (6)-(8) and (23) together imply that  $\mathcal{A}_{\perp}^{L,R}$  must have an expansion at least  $\mathcal{O}(\sqrt{\delta})$  higher compared to  $\mathcal{A}_{\parallel,0}^{L,R}$ . This is in agreement with Ref. [6]. Hence the leading term in  $F_L$  and  $F_{\parallel}$  must be  $\mathcal{O}(\delta^0)$ , whereas the leading term for  $F_{\perp}$  is  $\mathcal{O}(\delta)$ . The leading terms for the asymmetries,  $A_5$  and  $A_{\text{FB}}$ , are  $\mathcal{O}(\sqrt{\delta})$ . Thus, we expand the observables as follows:

$$F_L = \frac{1}{3} + F_L^{(1)}\delta + F_L^{(2)}\delta^2 + F_L^{(3)}\delta^3 \quad (25)$$

$$F_{\perp} = F_{\perp}^{(1)}\delta + F_{\perp}^{(2)}\delta^2 + F_{\perp}^{(3)}\delta^3 \quad (26)$$

$$A_{\text{FB}} = A_{\text{FB}}^{(1)}\delta^{1/2} + A_{\text{FB}}^{(2)}\delta^{3/2} + A_{\text{FB}}^{(3)}\delta^{5/2} \quad (27)$$

$$A_5 = A_5^{(1)}\delta^{1/2} + A_5^{(2)}\delta^{3/2} + A_5^{(3)}\delta^{5/2}, \quad (28)$$

where for each observable  $O$ ,  $O^{(n)}$  is the coefficient of the  $n^{\text{th}}$  term in the expansion. The polynomial fit to data is not based on inspirations from Heavy Quark Effective Theory (HQET) or any other theoretical assumption. A parametric fit to data is performed, so as to obtain the limiting values of the coefficients to determine the slope and second derivative of the observables at  $q_{\text{max}}^2$ . It should be noted that the form of polynomials are inadequate to describe the  $q^2$  dependent behavior of resonances. However, systematics of resonance effects has been studied [14] in detail validating the approach followed here.

The relation in Eq. (24) between form factors is expected to be satisfied in the large  $q^2$  region. Eq. (24) is naturally satisfied if it is valid at each order in the Taylor expansion of the form factors:

$$q^2 \frac{\tilde{\mathcal{G}}_{\lambda}}{\mathcal{F}_{\lambda}} = q_{\text{max}}^2 \frac{\tilde{\mathcal{G}}_{\lambda}^{(1)} + \delta(\tilde{\mathcal{G}}_{\lambda}^{(2)} - \frac{\tilde{\mathcal{G}}_{\lambda}^{(1)}}{q_{\text{max}}^2}) + \mathcal{O}(\delta^2)}{\mathcal{F}_{\lambda}^{(1)} + \delta\mathcal{F}_{\lambda}^{(2)} + \mathcal{O}(\delta^2)}. \quad (29)$$

We require only that the relation be valid up to order  $\delta$ . In order for Eq. (29) to have a constant value in the neighborhood of  $q_{\text{max}}^2$  up to  $\mathcal{O}(\delta)$ , we must have  $\mathcal{F}_{\lambda}^{(2)} = c\mathcal{F}_{\lambda}^{(1)}$  and  $(q_{\text{max}}^2 \tilde{\mathcal{G}}_{\lambda}^{(2)} - \tilde{\mathcal{G}}_{\lambda}^{(1)}) = c q_{\text{max}}^2 \tilde{\mathcal{G}}_{\lambda}^{(1)}$  where  $c$  is any constant. As discussed earlier,  $\text{P}_2 = \sqrt{2}\text{P}_1$  at  $q_{\text{max}}^2$ , hence, we must have  $\text{P}_2^{(1)} = \sqrt{2}\text{P}_1^{(1)}$ , where  $\text{P}_{1,2}^{(1)}$  are the coefficients of the leading  $\mathcal{O}(\sqrt{\delta})$  term in the expansion. However, the above argument implies that at the next order, we must also have  $\text{P}_2^{(2)} = \sqrt{2}\text{P}_1^{(2)}$ , since  $\mathcal{F}_{\lambda}^{(2)} = c\mathcal{F}_{\lambda}^{(1)}$ . This provides the needed input that together with Eq. (22) determines  $\text{P}_1^{(1)}$  purely in terms of observables.

The expressions for  $R_{\lambda}$  in the limit  $q^2 \rightarrow q_{\text{max}}^2$  are

$$R_{\perp}(q_{\text{max}}^2) = \frac{8A_{\text{FB}}^{(1)}(-2A_5^{(2)} + A_{\text{FB}}^{(2)}) + 9(3F_L^{(1)} + F_{\perp}^{(1)})F_{\perp}^{(1)}}{8(2A_5^{(2)} - A_{\text{FB}}^{(2)})\sqrt{\frac{3}{2}F_{\perp}^{(1)} - A_{\text{FB}}^{(1)2}}} \\ = \frac{\omega_2 - \omega_1}{\omega_2\sqrt{\omega_1 - 1}}, \quad (30)$$

$$R_{\parallel}(q_{\text{max}}^2) = \frac{3(3F_L^{(1)} + F_{\perp}^{(1)})\sqrt{\frac{3}{2}F_{\perp}^{(1)} - A_{\text{FB}}^{(1)2}}}{-8A_5^{(2)} + 4A_{\text{FB}}^{(1)} + 3A_{\text{FB}}^{(1)}(3F_L^{(1)} + F_{\perp}^{(1)})} \\ = \frac{\sqrt{\omega_1 - 1}}{\omega_2 - 1} = R_0(q_{\text{max}}^2) \quad (31)$$

where

$$\omega_1 = \frac{3}{2} \frac{F_{\perp}^{(1)}}{A_{\text{FB}}^{(1)2}} \quad \text{and} \quad \omega_2 = \frac{4(2A_5^{(2)} - A_{\text{FB}}^{(2)})}{3A_{\text{FB}}^{(1)}(3F_L^{(1)} + F_{\perp}^{(1)})}. \quad (32)$$

It should be noted that Eqs. (30)–(32) are derived only at  $q_{\text{max}}^2$ . However, even at the endpoint, the expressions depend on polynomial coefficients:  $F_L^{(1)}$  and  $F_{\perp}^{(1)}$  as well as  $A_{\text{FB}}^{(2)}$  and  $A_5^{(2)}$  which are not related by HQET. Hence, in our approach, corrections beyond HQET are automatically incorporated through fits to data.

In the absence of RH currents or other NP that treats the “ $\perp$ ” amplitude differently one would expect  $R_{\perp}(q_{\text{max}}^2) = R_{\parallel}(q_{\text{max}}^2) = R_0(q_{\text{max}}^2)$ . It is easily seen that the LHS of Eq. (16) is positive around  $q_{\text{max}}^2$  and since  $\zeta > 0$ , we must have  $R_{\perp} = R_{\parallel} = R_0 > 0$ . Since very large contributions from RH currents are not possible, as they would have been seen elsewhere,  $R_{\lambda}(q_{\text{max}}^2) > 0$  still holds and restricts  $\xi$  and  $\xi'$  to reasonably small values.

	$O^{(1)}(10^{-2})$	$O^{(2)}(10^{-3})$	$O^{(3)}(10^{-4})$
$F_L$	$-2.94 \pm 1.36$	$12.27 \pm 2.05$	$-5.73 \pm 0.72$
$F_{\perp}$	$6.83 \pm 1.75$	$-9.67 \pm 2.59$	$3.77 \pm 0.90$
$A_{\text{FB}}$	$-30.59 \pm 2.37$	$26.75 \pm 4.42$	$-4.00 \pm 1.83$
$A_5$	$-16.57 \pm 2.36$	$6.77 \pm 4.18$	$1.94 \pm 1.61$

TABLE I. Best fit and  $1\sigma$  errors of the coefficients of observables (in Eqs. (25)–(28)) obtained by fitting recent LHCb’s 14- bin measurements [15] as a function of  $q^2$  for the entire region.

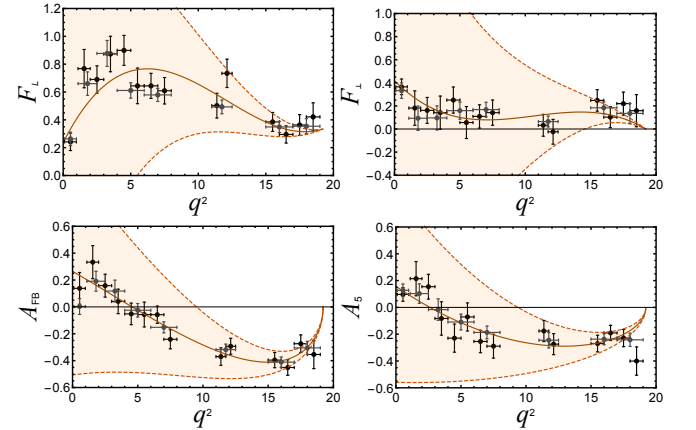


FIG. 1. An analytic fit to 14-bin LHCb data using Taylor expansion at  $q_{\text{max}}^2$  for the observables  $F_L$ ,  $F_{\perp}$ ,  $A_{\text{FB}}$  and  $A_5$  are shown as the brown curves. The  $\pm 1\sigma$  error bands are indicated by the light brown shaded regions. The points with the black and gray error bars are LHCb 14-bin and 8-bin measurements [15], respectively.

We fit the latest LHCb measurements [15] of the observables  $F_L$ ,  $F_{\perp}$ ,  $A_{\text{FB}}$  and  $A_5$  as functions of  $q^2$  using Taylor expansion at  $q_{\text{max}}^2$ . The fits were performed by minimizing the  $\chi^2$  function, which compares the bin integrated values of  $q^2$  functions of the observables with their measured experimental values for all 14 bins. The

bin integration for the polynomial fit is weighted with the recent measurements of differential decay rate [16]. We use the 14 bin data set based on the method of moments [17] from LHCb rather than the 8 bin data set as it enables better constraints near  $q_{\text{max}}^2$ . The best fit values for each coefficient of the observables  $F_L$ ,  $F_{\perp}$ ,  $A_{\text{FB}}$  and  $A_5$  (Eqs. (25)–(28)) are given in Table I. The errors in each coefficient are evaluated using a covariance matrix technique. A detailed study of the systematics in fitting the polynomial is described in Ref. [14]. Variations in the order of the polynomial from two to four and the number of bins used in fitting (from last four to fourteen), demonstrate good convergence when larger numbers of bins are considered.

In Fig. 1 the results of the fits for the observables  $F_L$ ,  $F_{\perp}$ ,  $A_{\text{FB}}$  and  $A_5$ , respectively, are compared with the measured LHCb data [15]. We notice that the factorization requirement  $A_{\text{FB}}^{(1)} = 2A_5^{(1)}$  holds to within  $\pm 1\sigma$ . We treat  $A_{\text{FB}}^{(1)}$  and  $2A_5^{(1)}$  as two independent measurements of the same quantity as we have neglected correlation between observables. We obtain  $\omega_1 = 1.09 \pm 0.33$  ( $0.93 \pm 0.36$ ) and  $\omega_2 = -2.87 \pm 6.69$  ( $-2.65 \pm 6.18$ ), where the first values are determined using  $A_{\text{FB}}^{(1)}$  and the values in the round brackets use  $2A_5^{(1)}$ .

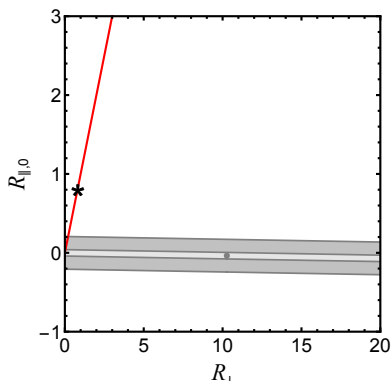


FIG. 2. Allowed regions in  $R_{\perp} - R_{\parallel,0}$  plane are shown. The solid red straight line on the far left corresponds to the case  $R_{\perp} = R_{\parallel,0}$ . The SM value is indicated by the star. The gray point corresponds to best fit central values. The light and dark gray contours correspond to  $1\sigma$  and  $5\sigma$  confidence levels.

We estimate the range of values for  $R_{\perp}$  and  $R_{\parallel,0}$  in two different ways. One approach estimates  $R_{\perp}$  and  $R_{\parallel,0}$  using randomly chosen values of  $F_L^{(1)}$ ,  $F_{\perp}^{(1)}$ ,  $A_{\text{FB}}^{(1)}$ ,  $A_5^{(1)}$ ,  $A_{\text{FB}}^{(2)}$  and  $A_5^{(2)}$ , from a Gaussian distribution with the central value as the mean and errors from Table I. If RH currents are absent the values would lie along a straight line with a  $45^\circ$  slope in the  $R_{\perp} - R_{\parallel,0}$  plane. However, we find a slope that is nearly  $0^\circ$ , indicating that  $R_{\perp} \gg R_{\parallel,0}$ . The deviation of slope from  $45^\circ$  provides evidence of contributions from RH currents.

In an alternate approach we fit the values of  $R_{\perp}$  and  $R_{\parallel,0}$  with the two estimated values of  $\omega_1$  and  $\omega_2$  by minimizing a  $\chi^2$  function. The allowed regions in the  $R_{\perp} - R_{\parallel,0}$  plane are shown in Fig. 2. The solid red straight line on the far left corresponds to the case  $R_{\perp} = R_{\parallel,0}$ . The SM value is indicated by the star on the red line. The light gray and dark gray contours denote the  $1\sigma$  and  $5\sigma$  permitted regions. We emphasize that for the SM, even in the presence of resonances the contours should be aligned along the  $45^\circ$  line, since resonances contribute equally to all helicities through  $\Delta C_9$  in Eq. (2). Hence the deviation of the contours from the SM expectation is a signal for RH currents. As discussed in [14], charmonium resonance contributions in bin averaged data always raise the values of  $\omega_1$ , whereas we find that the values of  $\omega_1$  are close to the lowest possible physical value allowed. In a study of resonance effects in  $B \rightarrow K\ell^+\ell^-$  [18], the difficulty in accommodating the LHCb-result in the standard treatment of the SM or QCD was noted and the possibility of right-handed current contributions was suggested.

Having established the existence of RH contributions, we perform a  $\chi^2$  fit to the parameters  $\xi$  and  $\xi'$  which indicate the size of the new Wilson coefficients. This is easily done using Eqs. (18), (30) and (31). However, this requires as an input the estimate of  $r/C_{10}$  from Eq. (24) at  $q_{\text{max}}^2$ . The allowed regions in the  $\xi - \xi'$  plane are shown in Fig. 3. The left panel shows the region obtained using SM estimate of  $r/C_{10} = 0.84$ . The best fit values of  $\xi$  and  $\xi'$ , with  $\pm 1\sigma$  errors are  $-0.83 \pm 0.82$  and  $-0.90 \pm 0.28$ , respectively. The yellow, orange and red bands denote  $1\sigma$ ,  $3\sigma$  and  $5\sigma$  confidence level regions, respectively. The SM value of  $C'_{10}/C_{10}$  and  $C'_9/C_{10}$  is indicated by the star, beyond the  $5\sigma$  confidence level contour. The SM estimate of  $r/C_{10}$  can have uncertainties that cannot easily be accounted for. These could range from errors in Wilson coefficients, contributions from other kinds of new physics or even the contributions from resonances. In order to ascertain the accuracy of our conclusion to these uncertainties, we have scanned [14]  $r/C_{10}$  over a range of values. While the evidence for right handed currents is clear, the central values of  $\xi$  and  $\xi'$  obtained from the fit can be reduced somewhat if  $r/C_{10}$  is smaller due to NP contributions that alter the Wilson coefficient  $C_9$  and the significance of discrepancy can also be reduced  $\sim 3\sigma$  as can be seen from Fig. 3 right panel plot. The value  $r/C_{10} = 0.6$  corresponds to the scenario in which NP contribution to the Wilson coefficient  $C_9$  is  $C_9^{\text{NP}} \approx -1$  as indicated by global fit analysis for  $b \rightarrow s$  transition [2]. In this case, best fit values of  $\xi$  and  $\xi'$  with  $\pm 1\sigma$  errors are  $-0.87 \pm 0.60$  and  $-0.67 \pm 0.27$ . We note that if  $\xi \neq 0$  is confirmed by further measurements, additional scalar and or pseudoscalar contributions would be needed in order to have consistency with  $B_s \rightarrow \mu^+\mu^-$  data [19].

We now incorporate the complex part of the transversity amplitudes i.e  $\varepsilon_\lambda$  contributions (in Eq. (3)), which

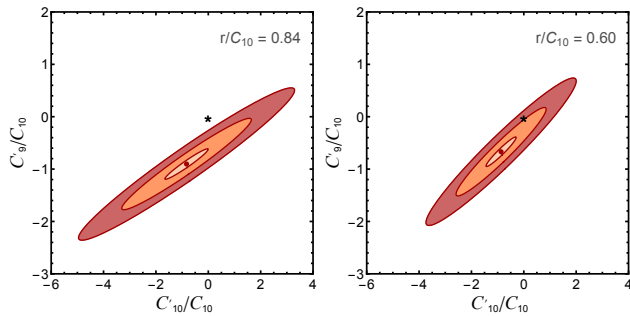


FIG. 3. Allowed regions in  $C'_{10}/C_{10} - C'_9/C_{10}$  plane are shown. The yellow, orange and red bands are the  $1\sigma$ ,  $3\sigma$  and  $5\sigma$  confidence level regions, respectively. The center red dot denotes best fit point; the SM values of  $C'_{10}/C_{10}$  and  $C'_9/C_{10}$  are indicated by a 'star', which sits more than  $5\sigma$  confidence level contour in the left panel and at  $3\sigma$  contour in the right panel. The plots illustrates the sensitivity to  $r/C_{10}$ . The left panel shows the SM value while the right panel includes an additional NP contribution  $C_9^{\text{NP}} \approx -1$  [2] (see text for details).

was not considered so far. In our approach  $\varepsilon_\lambda$  can be estimated at the endpoint purely from data. The  $\varepsilon_\lambda$  corrections do not contribute to the asymmetries  $A_{\text{FB}}$  and  $A_5$ , however, they do contribute to the helicity fractions  $F_L$  and  $F_\perp$  [7]. Interestingly, in a Taylor expansion of  $\hat{\varepsilon}_\lambda \equiv 2|\varepsilon_\lambda|^2/\Gamma_f$ , the coefficient of the leading term must be positive. We have used LHCb data to estimate  $\hat{\varepsilon}_0^{(0)}$ ,  $\hat{\varepsilon}_0^{(1)}$ ,  $\hat{\varepsilon}_\parallel^{(1)}$  and  $\hat{\varepsilon}_\perp^{(1)}$  that modify the estimates of  $\omega_1$  and  $\omega_2$ . We have also studied the effects of finite  $K^*$  width. Including these effects we find that our conclusions are very slightly strengthened [14].

In conclusion, we have shown how RH currents can be uniquely probed without any hadronic approximations at  $q_{\text{max}}^2$ . Our approach differs from other approaches that probe new physics at low  $q^2$ , as it does not require estimates of hadronic parameters but relies instead on heavy quark symmetry based arguments that are reliable at  $q_{\text{max}}^2$  [3, 4]. While the observables themselves remain unaltered from their SM values, their derivatives and second derivatives at the end point are sensitive to NP effects. Large values of  $A_{\text{FB}}$  and  $A_5$ , which do not rapidly approach zero in the neighborhood of  $q_{\text{max}}^2$ , are indicative of NP effects. We show that LHCb data implies  $5\sigma$  evidence

of NP at  $q_{\text{max}}^2$ . While the signal for right handed currents is clear, the large central values of  $\xi$  and  $\xi'$  obtained will be reduced if other NP contributions are present.

We thank Marcin Chrzszcz, Nicolla Serra and other members of the LHCb collaboration for extremely valuable comments and suggestions. We also thank B. Grinstein, N. G. Deshpande and S. Pakvasa for useful discussions. T. E. Browder thanks the US DOE for support.

- 
- [1] F. Kruger, L. M. Sehgal, N. Sinha, R. Sinha, Phys. Rev. **D61**, 114028 (2000). [hep-ph/9907386].
  - [2] W. Altmannshofer and D. M. Straub, Eur. Phys. J. C **75**, no. 8, 382 (2015); M. Ciuchini *et al.* JHEP **1606**, 116 (2016). S. Jager and J. Martin Camalich, Phys. Rev. D **93** (2016) 1, 014028; S. Descotes-Genon, L. Hofer, J. Matias and J. Virto, JHEP **1606**, 092 (2016) and references therein.
  - [3] B. Grinstein, D. Prijol, Phys. Rev. D **70** 114005 (2004).
  - [4] C. Bobeth, G. Hiller and D. van Dyk, Phys. Rev. D **87** (2013) 3, 034016
  - [5] R. Mandal and R. Sinha, arXiv:1506.04535 [hep-ph].
  - [6] G. Hiller, Roman Zwicky, JHEP **1403**, 042 (2014).
  - [7] R. Mandal, R. Sinha and D. Das, Phys. Rev. D **90**, no. 9, 096006 (2014)
  - [8] The lepton mass corrections can easily be included as shown in Ref. [7]. However the corrections are negligible at large  $q^2$ .
  - [9] M. Beneke, T. Feldmann, D. Seidel, Nucl. Phys. **B612**, 25-58 (2001). [hep-ph/0106067];
  - [10] A. Khodjamirian, T. Mannel, A. A. Pivovarov and Y.-M. Wang, JHEP **1009**, 089 (2010).
  - [11] W. Altmannshofer, P. Ball, A. Bharucha *et al.*, JHEP **0901**, 019 (2009). [arXiv:0811.1214 [hep-ph]].
  - [12] C. Bobeth, G. Hiller and D. van Dyk, JHEP **1007**, 098 (2010).
  - [13] D. Das and R. Sinha, Phys. Rev. D **86** (2012) 056006 [arXiv:1205.1438 [hep-ph]];
  - [14] Supplementary material.
  - [15] R. Aaij *et al.* [LHCb Collaboration], JHEP **1602**, 104 (2016).
  - [16] R. Aaij *et al.* [LHCb Collaboration], arXiv:1606.04731 [hep-ex].
  - [17] F. Beaujean, M. Chrzszcz, N. Serra and D. van Dyk, Phys. Rev. D **91**, 114012 (2015).
  - [18] J. Lyon and R. Zwicky, arXiv:1406.0566 [hep-ph].
  - [19] K. De Bruyn, R. Fleischer, R. Knegjens, P. Koppenburg, M. Merk, A. Pellegrino and N. Tuning, Phys. Rev. Lett. **109**, 041801 (2012) [arXiv:1204.1737 [hep-ph]].